



HAL
open science

Lake sediment mercury biogeochemistry controlled by sulphate input from drainage basin

Axel Canredon, Pierre Anschutz, Damien Buquet, Celine Charbonnier, David Amouroux, Emmanuel Tessier, Dominique Poirier, Stéphane Bujan, Ludovic Devaux, Benoit Guillieux, et al.

► To cite this version:

Axel Canredon, Pierre Anschutz, Damien Buquet, Celine Charbonnier, David Amouroux, et al.. Lake sediment mercury biogeochemistry controlled by sulphate input from drainage basin. *Applied Geochemistry*, 2019, 104, pp.135-145. 10.1016/j.apgeochem.2019.03.023 . hal-02282515

HAL Id: hal-02282515

<https://univ-pau.hal.science/hal-02282515>

Submitted on 22 Oct 2021

HAL is a multi-disciplinary open access archive for the deposit and dissemination of scientific research documents, whether they are published or not. The documents may come from teaching and research institutions in France or abroad, or from public or private research centers.

L'archive ouverte pluridisciplinaire **HAL**, est destinée au dépôt et à la diffusion de documents scientifiques de niveau recherche, publiés ou non, émanant des établissements d'enseignement et de recherche français ou étrangers, des laboratoires publics ou privés.



Distributed under a Creative Commons Attribution - NonCommercial 4.0 International License

1 **Lake sediment mercury biogeochemistry controlled by sulphate input from drainage basin**

2 Axel CANREDON¹, Pierre ANSCHUTZ^{1*}, Damien BUQUET¹, Céline CHARBONNIER¹, David
3 AMOUROUX⁴, Emmanuel TESSIER⁴, Dominique POIRIER¹, Stéphane BUJAN¹, Ludovic
4 DEVAUX^{1,3}, Benoît GOUILLIEUX², Sophie GENTES², Alexia LEGEAY², Agnès FEURTET-
5 MAZEL², Serge GALAUP⁵, Régine MAURY-BRACHET².

6 (1) Université de Bordeaux – CNRS, Environnements et Paléoenvironnements Océaniques et
7 Continentaux – EPOC, UMR5805, 33615 Pessac, France

8 (2) Université de Bordeaux – CNRS, Environnements et Paléoenvironnements Océaniques et
9 Continentaux – EPOC, UMR5805, Station Marine d'Arcachon, 2 Rue du Professeur Jolyet, 33120
10 Arcachon, France

11 (3) EPHE – Dynamique des Environnements Naturels et Anthropisés (DENA), UMR5805, 33615
12 Pessac, France

13 (4) CNRS – Université de Pau & Pays Adour, Institut des Sciences Analytiques et de Physico-chimie
14 pour l'Environnement et les Matériaux – IPREM, UMR5254, 64000, PAU, France.

15 (5) ENSEGID - Bordeaux INP, EA 4592 Géorressources & Environnement, 1 allée Daguin 33607
16 Pessac, France

17 (*), corresponding author, ORCID identifier is 0000-0001-5331-7974

18

19 ***Abstract***

20 Mercury (Hg) and methyl mercury (MeHg) concentrations have never been measured in
21 sediments of coastal lakes of Aquitaine, although high concentrations of Hg have been measured in
22 fish. Our objective was to characterize benthic biogeochemical processes and the distribution of Hg in
23 lake sediments and to connect these results with fish contamination. For this, we mapped and
24 characterized sediments. We measured sediment Hg and MeHg content, and biogeochemical
25 parameters. We identified organic deposits in deep areas, and sandy sediments in shallow areas.
26 Sediments were anoxic below the sediment–water interface. The average Hg concentration in organic

27 sediment was $213 \mu\text{g kg}^{-1}$ dry weight. Sandy sediments had an average Hg concentration of $4 \mu\text{g kg}^{-1}$
28 dw. We measured concentrations below $6 \mu\text{g kg}^{-1}$ dw in sediments from streams that drain the
29 catchment. Similar concentrations in the four lakes suggest that the source of total Hg was not a point
30 source in a given lake. The highest MeHg concentrations were found in the upper centimetres of
31 organic sediments, where sulphate reduction occurred. MeHg represented 2.53% of total Hg for Lake
32 Carcans-Hourtin, less in other lakes. The proportion of MeHg in sediment followed lake water
33 sulphate concentrations. High sulphate concentrations resulted from agricultural activity in the Lake
34 Carcans-Hourtin catchment. Our results corroborate the hypothesis that Hg methylation is linked to
35 sulphate-reducing activity. High fluxes of sulphate from a drainage basin may induce large proportions
36 of potentially bioavailable MeHg in lake sediment, even in non-polluted areas. The Hg methylation
37 activity in the sediment reflected the exposure of predatory fish to MeHg.

38

39 Keywords : Mercury methylation, fish contamination, aquatic sediment, sulphate, freshwater lake

40

41 ***1. Introduction***

42 Technological, industrial, and agricultural progress triggered both the exploitation of natural
43 resources and the dispersion of anthropogenic contaminants. Since the 19th century, mercury (Hg)
44 fluxes in the environment have increased at a global scale. Typical concentrations of Hg range from 50
45 to $150 \mu\text{g kg}^{-1}$ in the continental crust (Wedepohl, 1995), from 0.1 to 2 ng L^{-1} in continental and ocean
46 waters (Mason et al., 1994), and from 1 to 3 ng m^{-3} in the atmosphere (Schroeder and Munthe, 1998).

47 Mercury dynamics is characterizes by properties, such as volatility at ambient temperature,
48 stability of its bonds with carbon and sulphur, and very high bioconcentration and toxicity (Cossa and
49 Ficht, 1999). Methyl mercury (MeHg) is the most toxic chemical form of Hg. It is a neurotoxin for
50 vertebrates, which leads to damage in central nervous system (Allen et al., 2002). Methyl mercury
51 passes easily through biological barriers and can bioaccumulate and biomagnify along the food chain.
52 Although it is present at very low concentrations in water, it can concentrate up to 10 million times in
53 aquatic organisms such as predators (Cossa and Ficht, 1999). Human exposure to MeHg compounds

54 occurs often through the consumption of fish and fish products (Driscoll et al., 2013). High trophic
55 level species of fish can present very high MeHg concentrations. The maximum tolerable level for the
56 sale of carnivorous fish is 1 mg kg⁻¹ wet weight according to the European Commission directive
57 93/351/EEC.

58 Mercury is naturally emitted in the environment through degassing of the Earth's crust,
59 volcanoes, and erosion of soils and rocks. Human-related Hg emissions dominate the Hg cycle such
60 that most of the Hg in the atmosphere is anthropogenic (Mason et al., 1994). Natural Hg emission and
61 re-emission mainly occurs as elemental mercury vapours (Hg⁰). The main mercury source in aquatic
62 environments comes from wet and dry atmospheric deposition, and via runoff from the drainage basin
63 (Mason and Fitzgerald, 1996). Globally, the main anthropogenic Hg emissions into the atmosphere
64 originate from artisanal gold production, the combustion of coal, and solid wastes (Pirrone et al., 2010;
65 UNEP, 2013; Streets et al. 2017). These emissions, coupled with long-distance transport of elemental
66 Hg, result in a worldwide distribution of Hg deposition with a global average of 5.6 µg m⁻² yr⁻¹
67 (Lamborg et al., 2002).

68 In 2015, a large-scale sampling of piscivorous fish was conducted in order to study fish
69 contamination by mercury in the four main lakes in Aquitaine, specifically from the north to the south,
70 lakes Carcans-Hourtin, Lacanau, Cazaux-Sanguinet, and Parentis-Biscarrosse (Fig. 1). The results
71 showed an increasing Hg contamination gradient from Lake Parentis-Biscarrosse to Lake Carcans-
72 Hourtin (south–north gradient), with values in the top predator zander (*Sander lucioperca*) from 2000
73 µg kg⁻¹ dw in the southernmost lake to 7400 µg kg⁻¹ dw in the Lake Carcans-Hourtin (Gentès et al.,
74 submitted). This latter study showed that trophic transfer efficiency does not explain this Hg latitudinal
75 gradient in biota. The mercury concentration in fish suggested that the lakes underwent variable
76 contamination pressure. However, the four lakes are located in the same geological context, they are
77 subject to identical climate, and they do not have known local Hg sources, suggesting that different
78 fish contamination in each lake results from distinct methylation efficiency of a background Hg flux.
79 Therefore, these lakes represent a natural laboratory, in which the study of biogeochemical parameters
80 allows us to determine the impact of the main factors that control methylation of Hg. Methylation

81 occurs through the action of sulphate-reducing bacteria (Gilmour et al., 1992) and, to a lesser extent,
82 iron-reducing and methanogenic microorganisms (Alpers et al., 2013; Hamelin et al. 2011; Kerin et
83 al., 2006; Parks et al., 2013), which are common in organic-rich sediments. Consequently, methylation
84 is localized in the anoxic zone of aquatic environments such as biofilms, sediment, or water column.
85 As Aquitaine lakes are shallow, between 7 and 23 m maximum depth, the water column is generally
86 well mixed and oxygenated. Therefore, it was expected that anoxic conditions favourable to Hg
87 methylation occurred in anoxic sediments instead of the water column. Indeed, it has been observed
88 recently that the bottom of the deepest parts of Aquitaine lakes are blanketed with anoxic organic
89 muds (Buquet et al., 2017).

90 The present study focuses on the relationship between the biogeochemistry of lakes and the
91 distribution of mercury and MeHg in sediments. The aim was to (i) perform a mapping of lake
92 sediments in order to link Hg concentrations and the nature of the substrate, (ii) measure
93 concentrations of total mercury and methyl mercury in several representative sediment samples, (iii)
94 analyse the redox compounds influencing Hg speciation in sediments, (iv) attempt to explain the
95 differences in sediment mercury speciation between the four lakes studied, and finally (v) determine
96 the relationship of Hg in sediments and Hg in fish.

97

98

99 ***2. Materials and Methods***

100 **2.1. Study site**

101 Large lakes in Aquitaine are located close to the French Atlantic coast in the south-western
102 part of France. They are separated from the ocean by a 5-km-wide forested coastal dune system (Fig.
103 1), which represents a physical barrier to streams draining the lowland of Landes de Gascogne. Most
104 of the drainage basin of the lakes is located on the eastern side. The surface areas of the catchments are
105 similar, between 200 and 310 km² (Table 1), which is relatively small. The relief of the drainage
106 basins is very flat with an westward slope lower than 0.2%. The geology is homogeneous and consists

107 of podzols established on Quaternary siliceous aeolian deposits (Jolivet et al., 2007). Soil occupation
108 has been determined by remote sensing using maps of the French national institute of geography
109 (IGN), and aerial photographs analysed with the Geographic Information System (GIS) ArcGIS
110 (Canton et al., 2012). Pine (*Pinus pinaster*) forests dominate the land use and occupy more than 80%
111 of the total surface (Fig. 1). Intensive farming covers between 5% and 20% of lake drainage basins.
112 Housing is confined to the coastal zone.

113 Lakes are fed by direct rainfall on the lake surface and by low-discharge rivers. River systems
114 are artificial ditches dug to dry up marshes. Water level of lakes is controlled by locks in channels that
115 connect lakes. Locks also determine the water residence time (Table 1). Lake Lacanau is located
116 downstream from Lake Carcans-Hourtin. The lakes are connected by the 7.5-km-long Etang channel.
117 Waters of Lake Lacanau flow to the Arcachon Lagoon through the 18.5-km-long Porge channel. Lake
118 Parentis-Biscarrosse is downstream from Lake Cazaux-Sanguinet. All of these lakes are shallow (less
119 than 23 m) (Table 1). The deepest part is located on the western side of the lakes, at the base of the
120 dunes. Only the southern lakes are deep enough to have a marked summer thermocline at about 12 m
121 depth. The hypolimnion does not become totally anoxic in the oligotrophic Lake Cazaux-Sanguinet.
122 Cyanobacteria blooms occur frequently in Lake Parentis-Biscarrosse due to eutrophication caused by
123 the legacy of large amounts of phosphorus stored in lake sediment. This lake experiences short periods
124 of bottom-water anoxia for a few weeks during summer water stratification. Less than 10% of the
125 water volume becomes anoxic during these episodes. Dense stands of invasive aquatic plants (*Egeria*
126 *densa* and *Lagarosiphon major*) are found in Lake Parentis-Biscarrosse and Lake Lacanau. They are
127 developed in shallow-sheltered or deep-exposed areas and represent about 10% of lake surface area
128 (Bertrin et al., 2017). Only restricted vegetated areas occurs in the other two lakes. The highest
129 biomass is present in Lake Parentis-Biscarrosse, with an estimated amount of 2800 tons (Bertrin et al.,
130 2017).

131 **2.2.Sampling**

132 Fish were collected from the four lakes by fishing associations and federations and by a
133 professional fisherman during autumn 2015. Three well-represented piscivorous species in the four

134 lakes were selected: zander (*Sander lucioperca*), pike (*Esox Lucius*) and perch (*Perca fluviatilis*). They
135 were placed in zip-locked bags and immediately cooled at 4°C. Sampling of lake sediment was carried
136 out using cores and grabs. The sediment mapping of lakes was obtained from sediment grabs that were
137 deployed along high spatial resolution N–S and E–W transects (Fig. 2). This strategy allowed us to
138 collect samples from the different bathymetric levels. We collected the top 10 cm of sediment. We
139 obtained 70, 55, 59, and 60 homogenized sediment samples from Lakes Carcans-Hourtin, Lacanau,
140 Cazaux-Sanguinet, and Parentis-Biscarrosse, respectively. For Lake Cazaux-Sanguinet the sampling
141 location was constrained by the security perimeter of the Cazaux military base. Maps of the
142 distribution of sediment properties, such as organic carbon or Hg content, were obtained from
143 interpolation between grab and core samples, and bathymetry was used for extrapolation to map whole
144 lakes. Additional grabs have been collected to validate the sediment mapping based on bathymetry.

145 In addition, sediment cores allowed us to define the vertical distribution of reactive
146 compounds at the water–sediment interface. Sediment cores were collected at three to nine stations for
147 each lake. Stations were selected according to the sedimentary map established with sediment grabs.
148 Cores were collected in organic deposits and sandy sediments from each lake, and also in the
149 vegetated sediment of Lake Parentis-Biscarrosse. Some stations were sampled twice in two different
150 seasons; in April 2014 and in January 2015 for the two northern lakes, and in spring and summer 2016
151 for the two southern lakes. Bottom water in contact with sediment cores was always oxic. Core
152 sampling was carried out by scuba divers using 10-cm-diameter polycarbonate tubes. Sealed cores
153 were immediately brought to the shore and cut horizontally into several subsamples for pore water
154 extraction. Vertical subsampling and pore water extraction from lake sediment required specific
155 approaches. We distinguished broadly two kinds of sediment: sandy permeable sediments and very
156 fluid organic-rich muds. This latter sediment type was subsampled with a vertical resolution of 2 cm
157 using Tygon tubing connected to a 100-mL syringe. Sandy permeable sediment was collected using a
158 PVC tube pre-cut in the vertical dimension. The core was laid horizontally on its side and immediately
159 halved into two similar parts. The sediment was cut rapidly into 1- to 2-cm-thick slices. This technique
160 prevented the percolation of pore waters in the vertical dimension during subsampling. For each level
161 of sandy and muddy sediment, a subsample was immediately sealed in a pre-weighed clean vial and

162 frozen under an N₂-atmosphere for further analysis of the solid fraction and determination of water
163 content. Another subsample was put into a centrifuge vial.

164 Pore waters were extracted by centrifugation at 2100 g for 20 min under an inert N₂-
165 atmosphere. For muddy sediments, the supernatant was immediately filtered (0.2-µm cellulose acetate
166 syringe filter). For sandy sediments, we used 0.2-µm VivaSpin20 centrifuge vials (Anschutz and
167 Deborde, 2016). The possibility that traces of oxygen had affected the pore water concentrations of
168 reduced elements during the slicing and filtration could not be excluded. Our strategy to prevent
169 oxidation of reduced compounds was to handle the samples in less than 30 min from slicing to
170 conditioning. One part of filtered interstitial water was frozen at -18°C, and another part was acidified
171 with HCl at a pH close to 2 to measure dissolved manganese and iron. Soils of the Landes de
172 Gascogne forest were sampled to estimate the geochemical mercury background levels of the area.
173 Soils were collected every 5 cm from the surface to a depth of 1 m at three stations in young to mature
174 forests of the Lake Cazaux-Sanguinet watershed.

175 Lake water and stream waters of the drainage area were collected to measure dissolved
176 sulphate, Fe, and Mn (Buquet et al., 2017). A total of 13 streams were sampled every month in 2014
177 and 2015. Sampling locations were along roads parallel to the lakes at about 1 km from the east shore.
178 Samples were also collected in headwaters close to agricultural areas. Sediment from the beds of rivers
179 feeding the northernmost lakes was collected manually using 50-mL centrifuge tubes in order to
180 measure total mercury concentrations. Surface lake waters were sampled every month at several
181 stations using a 2-L Niskin bottle. Bottom waters were also sampled at deep stations, where cores were
182 collected on the western side of the lakes. More than 50 samples were collected for each lake. For
183 determination of dissolved sulphate, Fe, and Mn concentration, water was filtered in situ with 0.20-µm
184 cellulose acetate syringe filters. Filtered samples were stored in polypropylene tubes in a fridge after
185 acidification with HCl. Solutes were analysed within 3 weeks.

186 **2.3. Analyses**

187 *2.3.1. Fish*

188 Fish dissection was performed within 48 h in laboratory conditions. Dorsal muscle tissue free
189 of skin was dissected and frozen then freeze-dried and crushed. Based on the fact that size is correlated
190 with the age of the individuals, only zander between 50 and 70 cm (standard length), pike between 50
191 and 70 cm and perch between 18 and 23 cm were considered to compare Hg concentrations between
192 lakes.

193 2.3.2. *Solid fraction*

194 The grain-size distribution was measured using a Malvern laser diffraction particle size
195 analyser. For organic sediments, granulometry was carried out after organic matter removal with H₂O₂
196 to recover only the mineral particulate fraction. The bulk mineralogy was determined for this fraction
197 by X-ray diffraction using a Siemens D500 X-ray diffractometer with CuK α radiation (1.5405-Å
198 wavelength). Scans were done from 5° to 80° 2 θ at 0.02° s⁻¹, using a 40-kV accelerating voltage and
199 30-mA current. Peak identification and relative abundance estimates of minerals were determined
200 using EVA interpretation software and the DIFFRAC software package.

201 Particulate carbon and total sulphur were measured on freeze-dried samples by infrared
202 spectroscopy (LECO 200 C-S analyser). Organic carbon was measured after removal of carbonates
203 with 2 M HCl from 50 mg of powdered sample (Etcheber et al., 1999). The detection limit was 0.2‰
204 for carbon and 0.1‰ for sulphur. The precision of measurement was better than 5%. Ascorbate
205 solution was used to obtain the most reactive particulate Fe(III) and Mn(III,IV) fractions (Fe-asc, Mn-
206 asc) (Kostka and Luther, 1994). Iron and manganese content was analysed colorimetrically according
207 to standardized techniques (Anschutz and Deborde 2016) with \pm 5% precision.

208 Total mercury concentration was determined in 100 mg dry and crushed sediment and in fish
209 muscle by cold vapour atomic absorption spectrometry after incineration and amalgamation, using an
210 Advanced Mercury Analyser (Altec AMA 254). The Teflon grinding bowls for fish and the mortar for
211 sediments were washed with HCl 3% and rinsed with milli-Q water between each sample. The
212 analytical results were quality-checked by analysing international certified reference materials (IAEA
213 407 for fish and PACS-2 and MESS-3 for sediment) after each set of 10 samples. For this method,
214 precision was \pm 5% and the detection limit was 0.1 ng Hg.

215 Methyl mercury content in solid sediment was determined in samples of eight chosen cores
216 collected in winter or early spring, one organic sediment and one sandy sediment for each lake.
217 Measurements were performed by gas chromatography coupled to inductively coupled plasma mass
218 spectrometry (Trace Ultra GC-XII Series ICPMS, Thermofisher). Sample preparation and analytical
219 protocol were adapted from Bouchet et al. (2013) and Renedo et al. (2017). Mercury species were
220 extracted from 0.25 g of dry and crushed sediment in 5 mL of 6N ultrapure grade HNO₃ solution using
221 a microwave system (Discover SP-D, CEM). Digestion was achieved in CEM Pyrex vessels by 1 min
222 of warming up to 75 °C and 3 min at 75 °C with magnetic agitation to homogenize the samples. Prior
223 to GC injection, sample extracts were ethylated at pH 4 (NaBEt₄, 5% v:v, Merseburger
224 Spezialchemikalien), in order to produce volatile ethylated forms of Hg, then extracted in isooctane by
225 mechanical shaking (elliptic table, 20 min) and readily separated by gas chromatography.
226 Quantification was performed by species-specific isotope dilution by spiking known amounts and
227 concentrations of isotopically enriched standard solutions (MM²⁰¹Hg and ¹⁹⁹Hg(II), ISC) (Rodriguez
228 Martin-Doimeadios et al., 2004). The detection limit of the method was 0.03 ng Hg g⁻¹. The analytical
229 results were continuously quality-checked by analysing reference materials certified for Hg speciation
230 (IAEA-405 Estuarine Sediment). Relative standard deviation of MeHg concentration has been
231 evaluated to 1.7%, from triplicate preparations and analyses of the reference material.

232 2.3.3. *Dissolved compounds*

233 The sediment water content was determined from the weight difference between wet and dry
234 sediments. Dissolved iron (Fe²⁺) was analysed using the colorimetric method by adding a ferrozine
235 solution in an aliquot (Stookey, 1970). Dissolved manganese (Mn²⁺ and Mn³⁺) was determined
236 colorimetrically using a Cd–TCPP complex according to Madison et al. (2011). Dissolved Fe and Mn
237 were determined with ± 5% precision. Dissolved sulphate was analysed by a nephelometric method
238 based on BaSO₄ precipitation using BaCl₂ (Rodier, 1976). The detection limit was 10 µM, and the
239 precision of replicate samples was better than 8%.

240 **3. Results**

241 **3.1. Mercury in fish**

242 We observed the highest average total Hg concentrations in carnivorous fish from Lake Carcans-
243 Hourtin (Table 2), with a maximum value of 6.238 mg kg⁻¹ dw. Total Hg concentrations were two to
244 five times lower in fish collected from Lake Parentis-Biscarrosse. We measured intermediate values in
245 fish from Lake Lacanau and Lake Cazaux-Sanguinet. Therefore, the data revealed a decreasing
246 gradient from north to south for total Hg in piscivorous species.

247 **3.2. Sedimentary cover of lakes**

248 *3.2.1. Sediment mapping*

249 Sediment type was strongly influenced by bathymetry. Therefore, we used bathymetry to draw
250 the sediment map from the grab and core observations (Fig. 2). Deep areas in the western parts of the
251 lakes presented muddy deposits. These deposits had a homogeneous appearance and a very soft
252 consistency. The water content of this substrate was greater than 95%, making the sediment texture
253 very fluffy. These sediments were highly organic deposits. Organic deposits were found below 5 m
254 depth in lakes Carcans-Hourtin and Lacanau, below 7 m in Lake Cazaux-Sanguinet, and below 10 m
255 in Lake Parentis-Biscarrosse. For these two last lakes, deep areas also presented a mixture of these
256 organic deposits with sand, called sandy organic deposits or organic sands, depending on the
257 proportion of sand and organic carbon (Fig. 2). Organic sands were present in sub-lacustrine channels.
258 These channels are the paleo-valley of the rivers that flowed to the ocean before the formation of lakes
259 through the development of coastal dunes in the last thousand years (Buquet et al., 2017). Shallow
260 zones presented sands with shades of green, yellow, black, or grey depending on the content of iron
261 oxides or organic matter. The water content of sands was 20% in weight.

262 Vegetated areas of lakes Lacanau and Parentis-Biscarrosse consisted of sandy sediments. In sheltered
263 areas, 2 to 10 cm of muddy sediment covered the sand.

264 *3.2.2. Grain size*

265 Sand grain size after organic matter removal with H₂O₂ was very homogeneous, with a median
266 size of 362 μm, a standard deviation (SD) of 49 μm, and a standard error of the mean (s.e.) of 7 μm.
267 The sand was the same as the soils of the lake catchment (Fig. 3). The grain size of the mineral

268 fraction of organic deposits was centred between 10 and 20 μm (Fig. 3). X-ray diffraction indicated
269 that the mineral fraction consisted of quartz, clay minerals (illite and kaolinite), and feldspars.
270 Carbonate minerals were not detected.

271 3.2.3. *Total carbon and total sulphur*

272 Particulate organic carbon (POC) and total carbon (TC) measurements on grab and core
273 sediments gave the same concentration, indicating that TC consisted exclusively of POC and that
274 inorganic carbonate was absent or very scarce. TC concentration ranged from 10% to 30% in organic
275 deposits. Averaged TC concentrations (\pm SD) in organic sediments were 15.8% (\pm 3.1), 17% (\pm 1.4),
276 15.5% (\pm 1.7), and 15.2% (\pm 0.9) for lakes Carcans-Hourtin, Lacanau, Cazaux-Sanguinet, and
277 Parentis-Biscarrosse, respectively (Fig. 4). Concentrations ranged from 3% to 10% in sandy organic
278 deposits, and from 1% to 3% in organic sands. TC was below 1% in sands.

279 Total sulphur (TS) content was also dependent on the type of sediment. TS ranged from 1% to
280 4% in organic deposits (Fig. 4). The mean concentrations were close to 2.5% (\pm 0.8% SD) except for
281 organic sediments of Lake Parentis-Biscarrosse, in which the value was 1.2%. TS ranged from 0.1% to
282 1% in sandy organic deposits and organic sands. TS was below 0.1% in sands.

283 3.2.4. *Particulate total mercury (HgTp)*

284 HgTp concentrations were closely related to the nature of sediment and the organic carbon
285 concentrations. Classes of mercury concentration fitted classes of TC content (Fig. 2). HgTp
286 concentrations ranged from 100 to 420 $\mu\text{g kg}^{-1}$ in organic deposits (means of 230 (\pm 82 SD), 203 (\pm 60
287 SD) 206 (\pm 68 SD), and 142 $\mu\text{g kg}^{-1}$ (\pm 53 SD) for lakes Carcans-Hourtin, Lacanau, Cazaux-
288 Sanguinet, and Parentis-Biscarrosse, respectively). HgTp concentrations in Lake Parentis-Biscarrosse
289 were significantly lower (ANOVA test) than in other lakes (Fig. 4). HgTp concentrations ranged from
290 20 to 100 $\mu\text{g kg}^{-1}$ in sandy organic deposits. HgTp concentrations ranged from 4 to 20 $\mu\text{g kg}^{-1}$ in
291 organic sands. Finally, HgTp concentrations ranged from below the detection limit to 10 $\mu\text{g kg}^{-1}$ in
292 sands (Fig. 2).

293 3.2.5. *Geochemical background levels*

294 Sand samples from forest soil east of Lake Cazaux-Sanguinet had the same particle size
295 distribution as the sandy sediments from lakes (Fig. 3). HgTp concentrations ranged from 0.5 to 21 μg
296 kg^{-1} . Highest values were associated with soil samples enriched in organic carbon. However, HgTp
297 values were not significantly different (ANOVA test) in lake sands and in drainage basin soils (Fig. 2).
298 Fine sediments collected from the beds of streams that feed Lake Carcans-Hourtin and Lake Lacanau
299 had a mean HgTp concentration of $2.3 \pm 1.8 \mu\text{g kg}^{-1}$, which was much lower than values measured in
300 lake organic sediments.

301 **3.3. Lake sedimentary column**

302 Cores of organic deposits had a TC concentration between 10% and 30% (Fig. 1S,
303 Supplementary Material), like sediment grabs. TC decreased slightly with depth, except for Lake
304 Carcans-Hourtin, which showed a sharp decrease in TC below 10 cm depth from 30% to 15%. TS
305 concentrations were similar to values measured in grabs. Concentrations increased with depth, except
306 in organic muds of Lake Carcans-Hourtin, where sediments below 25 cm depth were less enriched in
307 sulphur than those above. Iron and manganese oxide concentrations extracted by leaching with
308 ascorbate decreased with depth. Ascorbate-extracted iron was two- to three-fold higher in muddy
309 sediments of Lake Parentis-Biscarrosse than in other lakes. HgTp concentrations were between 100
310 and 300 $\mu\text{g kg}^{-1}$ in organic sediments. Shallow vegetated sediment from Lake Parentis-Biscarrosse
311 contained up to 80 $\mu\text{g kg}^{-1}$ HgTp in the muddy layer of the superficial sediment. This muddy layer of
312 vegetated sediment contained about 10% TC.

313 Methylmercury concentrations of organic sediments were maximal in the first centimetres
314 below the water-sediment interface (Fig. 1S, Supplementary Material). There was an increasing
315 gradient in MeHg from the southern lakes to the northern lakes: average vertical concentrations in the
316 top 10 cm below the sediment-water interface were $4.61 (\pm 2.6 \text{ SD}) \mu\text{g kg}^{-1}$ for Lake Carcans-Hourtin,
317 $5.14 (\pm 2.8 \text{ SD}) \mu\text{g kg}^{-1}$ for Lake Lacanau, $1.56 (\pm 0.14 \text{ SD}) \mu\text{g kg}^{-1}$ for Lake Cazaux-Sanguinet, and
318 $1.1 (\pm 0.32 \text{ SD}) \mu\text{g kg}^{-1}$ for Lake Parentis-Biscarrosse, which represented 2.53% (± 1.0), 1.69% (\pm
319 0.7), 0.55% (± 0.1), and 0.53% (± 0.1) of HgTp, respectively.

320 Concentrations of TC, mercury, Fe and Mn oxyhydroxides, and sulphides were lower by a
321 factor of 10 to 100 in sandy sediment cores compared to muddy sediments. Contrary to observations
322 for organic sediments, mercury decreased with depth. MeHg concentrations were often below the
323 detection limit of the GC-ICPMS method (i.e. $0.03 \mu\text{g Hg kg}^{-1}$).

324 **3.4. Lake water and pore waters**

325 Sandy sediment depleted in organic carbon (e.g, Fig. 1S-A and 1S-G, Supplementary
326 Material) did not show a pronounced gradient of dissolved redox compounds below the sediment
327 surface, except a small sulphate decrease with depth. Pore water dissolved Fe and Mn remained at
328 concentrations similar to those measured in lake waters. Sandy sediments with an organic carbon
329 content above 0.5% showed more pronounced redox gradients, with appearance of reduced dissolved
330 species and rapid loss of sulphate in the first centimetres below the interface (Fig. 1S-H and 1S-J,
331 Supplementary Material). Dissolved iron and manganese concentrations were present from the first
332 centimetre of the sedimentary pore water column in cores that were collected in muddy sediments.
333 Dissolved sulphate concentrations decreased below the sediment surface in organic sediment pore
334 water to reach the detection limit a few centimetres below the interface. Dissolved sulphate
335 concentrations of overlying water differed depending on the lake. Mean water sulphate concentrations
336 were $328 (\pm 28 \text{ SD})$, $221 (\pm 26 \text{ SD})$, $100 (\pm 19 \text{ SD})$, and $82 (\pm 17 \text{ SD}) \mu\text{M}$ for lakes Carcans-Hourtin,
337 Lacanau, Cazaux-Sanguinet, and Parentis-Biscarrosse, respectively ($N > 50$ for each lake). Therefore,
338 there was a decreasing north–south gradient of sulphate concentrations. Mean dissolved sulphate
339 concentration of the stream waters that feed the lakes was lower than $150 \mu\text{M}$, except for the Lake
340 Carcans-Hourtin catchment, where streams contained up to $600 \mu\text{M}$ sulphate (Fig. 5). For this lake,
341 sulphate concentrations were the highest in head waters close to agricultural areas. Values above 1000
342 μM were measured in upstream waters of the Caillava river, which drain large maize fields (Fig. 5).
343 Head waters that drain maize fields of the Cazaux-Sanguinet catchment were also enriched in
344 dissolved sulphate, with mean concentrations of $300 \mu\text{M}$.

345 **4. Discussion**

346 **4.1. Mercury distribution, diagenetic processes, and mercury mobility in sediments**

347 *4.1.1. Mercury distribution and background concentrations*

348 The concentration of HgTp was close to 200 $\mu\text{g kg}^{-1}$ in organic muds and below 20 $\mu\text{g kg}^{-1}$ in
349 sandy sediments. Concentrations were below 2 $\mu\text{g kg}^{-1}$ in sands poor in organic carbon. Sandy
350 sediments had concentrations identical to those measured in forest sandy soil from the lake drainage
351 basin. Sands were deposited before the formation of Aquitaine lakes, whereas the fine particles present
352 in organic deposits were autochthonous sediments. Higher HgTp values in organic muds may result
353 from a grain-size effect: deep parts of lakes accumulate fine-grained particles that consist of fine
354 quartz and clay minerals, which are probably enriched in Hg relative to sandy sediments (Bloom and
355 Crecelius, 1987). However, grain size alone cannot explain the difference, because mercury has a
356 strong affinity with organic carbon, sulphur, and Fe/Mn oxides (Feyte et al., 2010), which are highly
357 enriched in muddy sediment. The difference in HgTp content between sands, sands enriched in
358 organic matter, and muds is most likely explained by the organic matter content (Fig. 2), suggesting
359 that organic matter is the initial carrier phase of Hg that accumulates in the sediment.

360 *4.1.2. Diagenetic processes*

361 Mercury has affinity with organic matter, iron/manganese oxyhydroxides, and sulphides.
362 Therefore, it is strongly influenced by diagenetic processes (Matty and Long, 1995). These processes
363 are directly linked to benthic organic matter mineralization. Mineralization of organic matter is the
364 result of its oxidation, carried out in presence of microorganisms, and is accompanied by reduction of
365 electron acceptors according to a sequence of reactions where O_2 is used preferentially, then nitrate
366 when the sediment becomes depleted in dissolved oxygen. In anoxic sediments, mineralization
367 consumes oxides and oxyhydroxides of manganese (MnO_2 , $\text{MnO}(\text{OH})$) and iron ($\text{Fe}(\text{OH})_3$) present in
368 the solid fraction of sediments, and dissolved sulphate (SO_4^{2-}) and CO_2 , which generally represent
369 both the main electron acceptors in anoxic environments (Stumm and Morgan, 1996). Anoxic
370 sediment is generally enriched in particulate sulphur because of the precipitation of sulphide minerals
371 as a result of sulphate reduction.

372 Redox species profiles in the cores (Fig. 1S, Supplementary Material) agreed with a typical
373 diagenetic sequence. Iron and manganese oxides extracted with an ascorbate solution have the highest
374 concentrations at the sediment surface and decrease with depth. Dissolved reduced iron and
375 manganese appear in the top core samples. This indicates that sediments are anoxic from the first
376 centimetre of the sediment column. Sulphate concentration decreases rapidly and reaches a value
377 below the detection limit a few centimetres below the sediment surface, which means that the sulphate
378 reduction process occurs effectively. Sulphide precipitate is produced as FeS, as suggested by the high
379 particulate S content in organic deposits and the decreasing pore water iron concentration with depth.
380 It must be noted that the concentration gradients in organic sediments are stronger than gradients in
381 sandy sediments, suggesting that diagenetic processes are more intense in muddy sediments. However,
382 the decrease and disappearance of sulphate in sandy cores suggest that the small amount of organic
383 matter present in sands is labile.

384 4.1.3. *Mercury diagenesis*

385 Mercury transformation in sediments depends on many biogeochemical processes, which may
386 affect the ability of mercury to be methylated, or to migrate from sediment to the water column
387 (Schäfer et al., 2010). Mercury mobility depends on its speciation between solid and dissolved phases.
388 This distribution is intimately coupled to organic matter mineralization as Hg distribution is influenced
389 by the presence of Mn/Fe oxyhydroxides and sulphide minerals. In oxic sediment layers, Hg mobility
390 is generally low because it is essentially associated with the solid phase by adsorption or precipitation
391 with Fe/Mn oxyhydroxides (Feyte et al., 2010). During the organic matter mineralization process,
392 Fe/Mn oxyhydroxides may be reduced, and associated Hg is released (Matty and Long, 1995). In the
393 sediment cores studied, the decrease in Fe/Mn oxyhydroxide concentrations with depth in lakes
394 Carcans-Hourtin, Lacanau, and Cazaux-Sanguinet can be interpreted as metal oxide reduction. In Lake
395 Parentis-Biscarrosse, the oxide concentration remains high in all organic cores, suggesting that Hg
396 mobility is limited in this lake. In anoxic sediments, sulphate reduction leads to sulphide production,
397 for which Hg has a strong affinity. Mercury precipitates as HgS or it is absorbed on FeS and included
398 in pyrite (Fitzgerald and Lamborg, 2003). Grab samples show that the Hg concentration increases

399 when total S concentration increases as well (Fig. 6). This trend also occurs in organic sediment cores.
400 Sulphur is associated with organic matter either as an initial compound or as a result of the
401 sulphurization by sulphide of organic matter during diagenesis (Urban et al., 1999). Therefore, high
402 organic matter concentrations correspond to high sulphur concentrations. Urban et al. (1999) found an
403 averaged C:S ratio of organic matter between 167 and 198 based on sediment cores from 50 lakes. For
404 lake sediments with the highest concentrations of organic carbon they found a maximum organic
405 sulphur concentration of $260 \mu\text{mol g}^{-1}$ (0.83%), which is below the concentration of sulphur measured
406 in muddy sediments (Fig. 6). This indicates that most of the sedimentary sulphur occurs as particulate
407 sulphide, and that particulate sulphides are major carrier phases of Hg in organic sediments. Organic
408 matter itself presents many adsorption sites for Hg, which plays a role in Hg mobility (Benoit et al.,
409 1998). This probably explains why organic sediments are enriched in Hg relative to organic-poor
410 sandy sediments (Fig. 2). Organic matter is mineralized in sediments through early diagenesis
411 processes. In anoxic lake sediments, Hg initially trapped in the fraction of organic matter that is
412 consumed is most likely released into the interstitial waters and then quickly trapped by sulphides
413 when sulphate reduction occurs (Benoit et al., 1999).

414 **4.2. Methylation**

415 *4.2.1. Vertical distribution*

416 Organic sediments of Lake Carcans-Hourtin and Lake Lacanau show the highest
417 concentrations of MeHg at the depth where the decreasing gradient of dissolved sulphate occurs.
418 Inorganic Hg methylation takes place during Hg(II) absorption by some anaerobic microorganisms
419 which methylate Hg in their cytoplasm (Benoit et al., 1999; Gilmour et al., 1998). Microbial sulphate
420 reduction (MSR) is recognized to be the most common pathway leading to mercury methylation in
421 sediments (Barkay and Wagner-Döbler, 2005; Compeau and Bartha, 1985). Other anaerobic
422 microorganisms such as iron-reducing bacteria are able to methylate Hg (Podar et al., 2015).
423 Diagenetic profiles of organic cores show that anaerobic processes occur at the depth of the maximum
424 MeHg concentrations (Fig. 1S, Supplementary Material). This suggests that the predominant process
425 of mercury methylation is carried out by a consortium of anaerobic microorganisms, including those

426 involved in MSR. Communities of Fe- and sulphate-reducing bacteria are also involved in MeHg
427 demethylation processes (Oremland et al., 1991; Bouchet et al., 2013). It is the balance between
428 methylation and demethylation in sediment that dictates the standing pool of MeHg (Rodríguez
429 Martín-Doimeadios et al., 2004). The progressive decrease in MeHg with depth of the sedimentary
430 column could be related to the dominance of demethylation processes in the deep sediment, when
431 sulphate becomes depleted (Pak and Bartha 1998).

432 4.2.2. *Spatial distribution*

433 Organic sediments of the four lakes have different MeHg concentrations. The fraction of total
434 Hg present as MeHg (%MeHg) describes a positive south–north gradient from 0.5% in Lake Parentis-
435 Biscarrosse to 2.5% in Lake Carcans-Hourtin (Fig. 7). The proportions between 0.5% and 0.6%
436 obtained in the southernmost lakes are consistent with those found in the literature for lacustrine or
437 coastal systems (Table 3). Generally, MeHg concentration in sediment is less than 1% of HgTp (Morel
438 et al., 1998). MeHg proportions in northern lake sediments are high (especially Lake Carcans-
439 Hourtin), which means that the methylation potential is high in these lake sediments.

440 Main factors that are known to influence the methylation rate are Hg(II) availability and
441 bacteria activity within the sedimentary column. Sulphate inputs stimulate MSR activity. As sulphate
442 concentrations differ between lakes, the high proportion of MeHg in northern lakes, more particularly
443 in Lake Carcans-Hourtin, can be related to high methylation potential as sulphate concentrations are
444 the highest (Fig. 7). Previous studies have found that sulphate addition stimulates net methylation rates
445 in fresh water sediments (e.g, Gilmour et al. 1992; Åkerblom et al. 2013). Sulphide from sulphate
446 reduction is known to have two effects on the availability of Hg(II). At low concentrations, sulphide
447 promotes methylation. By contrast, for higher concentrations, as may be the case in marine sediments,
448 sulphide limits the bioavailability of Hg(II) to be methylated (Benoit et al., 1998; Hsu-Kim et al.,
449 2013; Johnson et al., 2016). This suggests that there is a range of sulphate concentration which is
450 optimal for Hg methylation, above which methylation is inhibited. A broad range in the sulphate
451 concentration associated with maximum efficiency of Hg methylation has been observed. For
452 example, Orem et al. (2014) observed maximum MeHg concentrations at sulphate concentrations of 2

453 and 10–15 mg L⁻¹ in the Everglades Protection Area. Peak MeHg was observed in wetland mesocosms
454 with a sulphate concentration of 59 and 93 mg L⁻¹ (Myrbo et al., 2017). In the case of Aquitaine lake
455 muddy sediments, MeHg concentrations increase with sulphate, suggesting that MSR is not limited,
456 and that produced sulphide does not inhibit Hg availability. The availability of dissolved sulphide
457 produced by MSR will depend on iron oxide availability. The reactive fraction of iron oxides
458 determined by the ascorbate reagent is above 100 μmol g⁻¹ in the surface sediments of the four lakes,
459 which represents at least, when considering sediment water content, 4000 μmol L⁻¹, suggesting that
460 the sulphide produced is efficiently trapped as Fe sulphide phases with this abundant available reactive
461 Fe.

462 Temperature is an important control factor for methylation process. Low temperatures will
463 slow down methylation (Hintelmann and Wilken, 1995; Ramlal et al., 1993). The cores studied were
464 sampled in different seasons, but MeHg was measured only in cores collected in winter and early
465 spring. Higher concentrations of MeHg in summer may be expected, although the effect of
466 temperature on biotic demethylation is not well known. Gradients of dissolved sulphate between the
467 water column and the sediment were sharper when the water temperature was the highest at a given
468 station sampled in two seasons, suggesting that the sulphate reduction rate, and the related
469 methylation, was more efficient in summer and autumn.

470 The gradient of mercury contamination in carnivorous fish muscles between the four lakes
471 (Table 2) fits well with sediment MeHg concentrations, since the highest levels were measured in fish
472 from northern lakes. Therefore, the muddy sediment compartment may be one of the main sources of
473 MeHg which accumulates in the trophic chain (e.g. Hammerschmidt et al., 2004). Periphyton
474 microbial communities of aquatic macrophytes of Lake Cazaux-Sanguinet have also been recognized
475 to potentially methylate Hg (Gentès et al., 2013). This study was based on experimental batches placed
476 under high environmental Hg concentrations and anoxic conditions. Hence, through dietary
477 bioaccumulation, the MeHg in higher trophic levels within Aquitaine lakes may be attributed to MeHg
478 produced in anoxic muds, as observed in the present study and in the periphyton (Gentès et al., 2013),
479 both being limited by sulphate.

480 Sulphate from lake waters may originate from several sources: atmospheric inputs from rain
481 and ocean spray, rocks from the drainage area, and anthropogenic inputs. The distance from lake to
482 ocean is the same for the four lakes studied, suggesting that the atmospheric sources by spray are
483 similar. The lake catchment geology is also the same for the four lakes. The major difference between
484 lake catchments is the land use. The drainage area of Lake Carcans-Hourtin has the highest proportion
485 of agriculture areas (Fig. 1). Tributaries of this lake are enriched in dissolved sulphate, with a
486 concentration as high as 1200 μM in ditches located upstream, in the cultivated areas (Fig. 6). Head
487 waters collected in ditches close to agriculture surfaces of the Lake Cazaux-Sanguinet catchment are
488 enriched in dissolved sulphate compared to waters collected downstream, but the concentrations
489 remain below 300 μM . Thus, agricultural activity is the main source of sulphate. Discussions with
490 farmers informed us of the fact that sulphate was supplied indirectly to croplands through liming,
491 which allows control of soil pH. Lime comes from limestone or dolomite quarries, and in some cases
492 in the recent past from neighbouring paper mill plants that produce lime sludge as a by-product.
493 Depending on lime origin, the sulphate content can be high, and lime can become a source of sulphate
494 for lakes.

495 4.2.3. *MeHg diffusion and bioavailability*

496 Our study points out that MeHg concentration is related to sulphate concentration. Methyl
497 mercury produced in the sediment can be transferred to the water column through molecular diffusion
498 and resuspension of surface sediments. Hence, the amount of MeHg diffusing into the water column
499 and thus the amount bioavailable to pelagic organisms depends, among other things, on the proportion
500 of lake floor carpeted with organic sediments. Organic deposits account for 21%, 20%, 19%, and 18%
501 of the surface area of lakes Carcans-Hourtin, Lacanau, Cazaux-Sanguinet, and Parentis-Biscarrosse,
502 respectively. These proportions are close and suggest that the proportion of organic sediment is not the
503 variable that explains the gradient of fish contamination. Bioturbation and bioirrigation may affect the
504 transport of Hg from sediment to water (Benoit et al., 2006). We observed the presence of chironomid
505 larvae in some grabs from the four lakes. The density of these organisms was low, with zero to three
506 individuals per grab. Even if the density of benthic organisms was low, burrowing organisms may

507 assimilate MeHg directly from underlying anoxic sediments and become vectors of MeHg to pelagic
508 predators (Gagnon et al., 1996). Finally, despite the occurrence of episodic bottom-water anoxia
509 during the summer in Lake Parentis-Biscarrosse, this lake remains the one in which the fish are less
510 contaminated with Hg. The methylation of Hg in a polymictic lake can be shifted from the sediment to
511 the anoxic water column, because sulphate reduction is shifted in the same way to the water column
512 (Ramlal et al., 1993; Wartras et al., 1995). This suggests that sulphate availability remains a key
513 environmental parameter for Hg methylation, wherever sulphate reduction occurs, in the water column
514 or at the sediment surface.

515 **4.3. Sources of Hg**

516 Land use is not impacted by activities that may represent point sources of Hg. HgTp
517 concentrations are similar in lake sandy sediments and in watershed sandy soils, with values below 20
518 $\mu\text{g kg}^{-1}$, suggesting that the geological background level is low. Moreover, we measured HgTp
519 concentrations of between 1 and 7 $\mu\text{g kg}^{-1}$ in fine sediments of river beds, which is low compared to
520 the 200 $\mu\text{g kg}^{-1}$ measured in lakes muds, suggesting that the contribution of Hg from lake catchment is
521 negligible. Hg distribution in lakes depends exclusively on sediment type, not on geography: there is
522 no zone that presents a peak of HgTp concentration. This suggests the absence of a point source in
523 lakes. Several lines of evidence suggest that Hg that accumulates in muddy sediment is mainly of
524 atmospheric origin. Considering that the superposition principle applies to organic sediment deposits,
525 the decrease in Hg concentrations when approaching the water–sediment interface (Fig. 1S,
526 Supplementary Material) may be explained by the decrease in atmospheric emission in European
527 countries in recent decades (UNEP, 2013).

528 South-western France is not a hot spot for atmospheric Hg emissions (Colette et al., 2016). In
529 the light of the concentrations measured in lake sediments, Hg fluxes are not alarming. Average
530 atmospheric Hg flux on the Aquitaine coast is estimated by modelling as 10 $\mu\text{g m}^{-2} \text{yr}^{-1}$ for the year
531 2001 (Roustan et al., 2006). Such a flux represents 620, 200, 580, and 350 g yr^{-1} for lakes Carcans-
532 Hourtin, Lacanau, Cazaux-Sanguinet, and Parentis-Biscarrosse, respectively. Considering that all Hg
533 that reaches the lake surface is trapped in organic matter that accumulates in organic sediments,

534 considering also the mean HgTp of each lake and the particle content of organic sediment (40 g L^{-1}),
535 we found that 1 cm of deposit contains between 1 and 1.8 years of Hg deposition. This suggests that
536 the mean sedimentation rate is between 0.6 and 1.0 cm yr^{-1} . A very similar value was found for lakes
537 Lacanau and Carcans-Hourtin using a mass balance based on dissolved inorganic nitrogen retention
538 (Buquet et al., 2017). The higher sedimentation rate found here (1 cm yr^{-1}) is for Lake Parentis-
539 Biscarrosse. This lake has a higher phosphorus content than the other lakes (Cellamare et al., 2011),
540 which results in higher primary production. Eutrophication of the lake may explain a higher
541 sedimentation rate of organic matter. As a consequence, the concentration of HgTp is lower in the
542 muds of Lake Parentis-Biscarrosse than that of other lakes, even if the atmospheric flux is the same,
543 due to a dilution effect.

544 **5. Conclusion**

545 Our study presents new results from Aquitaine lake sediments. We have established the first
546 map of sediment distribution and we have determined several physicochemical properties of these
547 sediments. More particularly, we showed that the bottom of the four lakes consists of sands. Sandy
548 sediments are covered with organic muds, which accumulate only in the deepest parts of lakes and in
549 shallow densely vegetated areas. The highest Hg concentrations are encountered in these organic
550 deposits. However, they do not exceed reference thresholds for sediments ($1100 \mu\text{g kg}^{-1}$ for the
551 probable effect concentration; MacDonald et al., 2000). Organic sediment traps Hg in the four lakes,
552 which is most likely of background diffusive atmospheric origin. These sediments are hot spots for Hg
553 methylation, due to sulphate reduction processes.

554 The mercury concentration gradient in the muscles of carnivorous fish is the same as the
555 methyl mercury concentration gradient of lake sediment. This suggests that the sedimentary
556 compartment could be a MeHg source for the water column, resulting in its accumulation along the
557 trophic chain. Methylation rate depends on sulphate reduction activity. This activity is limited by
558 sulphate availability. Lake Carcans-Hourtin is the most concentrated in sulphate. Lake Lacanau, whose
559 waters come partly from Lake Carcans-Hourtin, is enriched in sulphate by this very fact. Agricultural
560 activity is the main source of sulphate in the Lake Carcans-Hourtin drainage basin. This excess

561 sulphate that is leached from soils instead of being absorbed and exported by plants originates likely
562 from liming. Therefore, the use of sulphate-rich lime in the headwater drainage area has an indirect
563 consequence on carnivorous fish Hg content in lakes located at the outlet of the catchment, because
564 sulphate favours methylation of the background flux of atmospheric Hg in anoxic environments of
565 lakes, such as autochthonous organic sediments, as seen in this study, or in other compartments, such
566 as aquatic plant periphyton (e.g. Gentès et al., 2013). One question that remains unresolved focuses on
567 the pathway that transmits MeHg produced from the sediment to fish. For that the distribution of Hg in
568 fish and in the food web is presently conducted in Aquitaine lakes.

569

570 ***Acknowledgements***

571 We thank Cécile Bossy, Lionel Dutruch, Rémy Sinays, and Thierry Corrège for their assistance
572 during field and laboratory work. We acknowledge the assistance given by Frank Quenault. This
573 research was founded by the project CLAQH (Agence de l'eau Adour-Garonne, Région Nouvelle
574 Aquitaine), the Syndicat Intercommunal d'Aménagement des Eaux du Bassin Versant des Etangs du
575 Littoral Girondin (SIAEBVELG), the LITTOLAC project supported by the French national program
576 INSU-EC2CO-BIOHEFECT, and the project PSDR AQUAVIT (Région Nouvelle Aquitaine and
577 INRA). This study has been carried out in the frame of the Investments for the future Program, within
578 the Cluster of Excellence COTE (ANR-10-LABEX-45).

579

580 ***References***

- 581 Åkerblom, S., Bishop, K., Björn, E., Lambertsson, L., Eriksson, T., Nilsson, M.B., 2013., Significant interaction
582 effects from sulfate deposition and climate on sulfur concentrations constitute major controls on
583 methylmercury production in peatlands. *Geochim. Cosmochim. Acta* 102: 1–11.
- 584 Allen, J.W., Shanker, G., Tan, K.H., Aschner, M., 2002. The consequences of methylmercury exposure on
585 interactive functions between astrocytes and neurons. *NeuroToxicology* 23: 755–759.
- 586 Alpers, C.N., Fleck, J.A., Marvin-DiPasquale, M., Stricker, C.A., Stephenson, M., Taylor, H.E., 2013. Mercury
587 cycling in agricultural and managed wetlands, Yolo Bypass, California: spatial and seasonal variations
588 in water quality. *Sci. Total Environ.* 484: 276–287.

589 Anschutz, P., Deborde, J., 2016. Spectrophotometric determination of phosphate in matrices from sequential
590 leaching of sediments. *Limnol. Oceanogr. Methods* 14: 245–256.

591 Avramescu, M.L., Yumvihoze, E., Hintelmann, H., Ridal, J., Fortin, D.R.S., Lean, D., 2011. Biogeochemical
592 factors influencing net mercury methylation in contaminated freshwater sediments from the St.
593 Lawrence River in Cornwall, Ontario, Canada. *Sci. Total Environ.* 409: 968–978.

594 Barkay, T., Wagner-Döbler, I., 2005. Microbial transformations of mercury: potentials, challenges, and
595 achievements in controlling mercury toxicity in the environment. *Adv. Appl. Microbiol.* 57:1–52

596 Benoit, J.M., Gilmour, C.C., Mason, R.P., Heyes, A., 1999. Sulfide controls on mercury speciation and
597 bioavailability to methylating bacteria in sediment pore waters. *Environ. Sci. Technol.* 33: 951–957.

598 Benoit, J.M., Gilmour, C.C., Mason, R.P., Riedel, G.S., Riedel, G.F., 1998. Behavior of mercury in the Patuxent
599 River estuary. *Biogeochemistry* 40: 249–265.

600 Benoit, J.M., Shull, D.H., Robinson, P., Ucran, L.R., 2006. Infaunal burrow densities and sediment
601 monomethylmercury distributions in Boston Harbor, Massachusetts. *Mar. Chem.* 102:124–133.

602 Bertrin, V., Boutry, S., Jan, G., Ducasse, G., Grigoletto, F., Ribaudou, C., 2017. Effects of wind-induced sediment
603 resuspension on distribution and morphological traits of aquatic weeds in shallow lakes. *J. Limnol.*
604 76(s1) <https://doi.org/10.4081/jlimnol.2017.1678>

605 Bloom, N.S., Crecelius, E.A., 1987. Distribution of silver, mercury, lead, copper and cadmium in central puget
606 sound sediments. *Mar. Chem.* 21: 377–390.

607 Bouchet, S., Amouroux, D., Rodriguez-Gonzalez, P., Tessier, E., Monperrus, M., Thouzeau, G., Clavier, J.,
608 Amice, E., Deborde, J., Bujan, S., Grall, J., Anschutz, P., 2013. MeHg production and export from
609 intertidal sediments to the water column of a tidal lagoon (Arcachon Bay, France). *Biogeochemistry*
610 114: 341–358.

611 Bowles, K.C., Apte, S.C., Maher, W.A., Kawei, M., Smith, R., 2001. Bioaccumulation and biomagnification of
612 mercury in Lake Murray, Papua New Guinea. *Can. J. Fish. Aquat. Sci.* 58: 888–897.

613 Buquet, D., Anschutz, P., Charbonnier, C., Rapin, A., Sinays, R., Canredon, A., Bujan, S., Poirier, D., 2017.
614 Nutrient sequestration in Aquitaine lakes (S France) limits nutrient flux to the coastal zone. *J. Sea Res.*
615 130: 24–35

616 Canton, M., Anschutz, P., Coynel, A., Polsenaere, P., Auby, I., Poirier, D., 2012. Nutrient export to an eastern
617 Atlantic coastal zone: First modeling and nitrogen mass balance. *Biogeochemistry* 107: 361–377.

618 Castelle, S., 2008. Spéciation et réactivité du mercure dans le système fluvio-estuarien Girondin. Thesis,
619 University Bordeaux 1.

620 Cellamare, M., Morin, S., Coste, M., Haury, J., 2011. Ecological assessment of French Atlantic lakes based on
621 phytoplankton, phytobenthos and macrophytes. *Environ. Monit. Assess.* 184: 4685–4708.

622 Colette, A., Aas, W., Banin, L., et al., 2016. Air pollution trends in the EMEP region between 1990 and 2012.
623 Joint Report of the EMEP Task Force on Measurements and Modelling (TFMM), Chemical Co-
624 ordinating Centre (CCC), Meteorological Synthesizing Centre-East (MSC-E), Meteorological
625 Synthesizing Centre-West (MSC-W). Kjeller, NILU (EMEP: TFMM/CCC/MSC-E/MSC-W Trend
626 Report) (EMEP/CCC, 01/2016).

627 Compeau, G.C., Bartha, R., 1985. Sulfate-reducing bacteria: principal methylators of mercury in anoxic
628 estuarine sediment. *Appl. Environ. Microbiol.* 50 : 498–502.

629 Cossa, D., Ficht, A., 1999. La dynamique du mercure. Editions Quae, Versailles.

630 Driscoll, C.T., Mason, R.P., Chan, H.M., Jacob, D.J., Pirrone, N., 2013. Mercury as a global pollutant: Sources,
631 pathways, and effects. *Environ. Sci. Technol.* 47: 4967–4983.

632 Etcheber, H., Relexans, J.C., Beliard, M., Weber, O., Buscail, R., Heussner, S., 1999. Distribution and quality of
633 sedimentary organic matter on the Aquitanian margin (Bay of Biscay). *Deep Sea Res. Part II Top. Stud.*
634 *Oceanogr.* 46: 2249–2288.

635 Feyte, S., Tessier, A., Gobeil, C., Cossa, D., 2010. In situ adsorption of mercury, methylmercury and other
636 elements by iron oxyhydroxides and organic matter in lake sediments. *Appl. Geochem.* 25: 984–995.

637 Fitzgerald, W.F., Lamborg, C.H., 2003. Geochemistry of mercury in the environment. *Treatise on Geochemistry*
638 9, Elsevier, pp 107–148.

639 Fleck, J.A., Marvin-DiPasquale, M., Eagles-Smith, C.A., Ackerman, J.T., Lutz, M.A., Tate, M., Alpers, C.N.,
640 Hall, B.D., Krabbenhoft, D.P., Eckley, C.S., 2016. Mercury and methylmercury in aquatic sediment
641 across western North America. *Sci. Tot. Environ.* 568 : 727–738.

642 Gagnon, C., Pelletier, E., Mucci, A., Fitzgerald, W.F., 1996. Diagenetic behavior of methylmercury inorganic-
643 rich coastal sediments. *Limnol. Oceanogr.* 41, 428–434.

644 Gentes, S., Monperrus, M., Legeay, A., Maury-Brachet, R., Davail, S., Andre, J.M., Guyoneaud, R., 2013.
645 Incidence of invasive macrophytes on methylmercury budget in temperate lakes: Central role of
646 bacterial periphytic communities. *Environ. Pollut.* 172: 116–123.

647 Gilmour, C.C., Henry, E.A., Mitchell, R., 1992. Sulfate Stimulation of mercury methylation in freshwater
648 sediments. *Environ. Sci. Technol.* 26: 2281–2287.

649 Gilmour, C.C., Riedel, G.S., Ederington, M.C., Bell, J.T., Gill, G.A., Stordal, M.C., 1998. Methylmercury
650 concentrations and production rates across a trophic gradient in the northern Everglades.
651 *Biogeochemistry* 40: 327–345.

652 Guédron, S., Point, D., Acha, D., Bouchet, S., Baya, P.A., Tessier, E., Monperrus, M., Molina, C.I., Groleau, A.,
653 Chauvaud, L., Thebault, J., Amice, E., Alanoca, L., Duwig, C., Uzu, G., Lazarro, X., Bertrand, A.,
654 Bertrand, S., Barbraud, C., Delord, K., Gibon, F.M., Ibanez, C., Flores, M., Fernandez Saavedra, P.,
655 Ezpinoza, M.E., Heredia, C., Rocha, F., Zepita, C., Amouroux, D., 2017. Mercury contamination level
656 and speciation inventory in Lakes Titicaca & Uru-Uru (Bolivia): Current status and future trends.
657 *Environ. Pollut.* 231: 262-270.

658 Hamelin, S., Amyot, M., Barkay, T., Wang, Y., Planas, D., 2011. Methanogens: principal methylators of
659 mercury in lake periphyton. *Environ Sci Technol* 45: 7693–7700.

660 Hammerschmidt, C.R., Fitzgerald, W.F., Lamborg, C.H., Balcom, P.H., Visscher, P.T., 2004. Biogeochemistry
661 of methylmercury in sediments of long island sound. *Mar. Chem.* 90: 31–52.

662 Hintelmann, H., Wilken, R.D., 1995. Levels of total mercury and methylmercury compounds in sediments of the
663 polluted Elbe River: influence of seasonally and spatially varying environmental factors. *Sci. Total*
664 *Environ.* 166 : 1–10.

665 Hsu-Kim, H., Kucharzyk, K.H., Zhang, T., Deshusses, M.A., 2013. Mechanisms regulating mercury
666 bioavailability for methylating microorganisms in the aquatic environment: A critical review. *Environ.*
667 *Sci. Technol.* 47 : 2441–2456.

668 Johnson, N.W., Mitchell, C.P., Engstrom, D.R., Bailey, L.T., Coleman Wasik, J.K., Berndt, M.E., 2016.
669 Methylmercury production in a chronically sulfate-impacted sub-boreal wetland. *Environ. Sci.:*
670 *Processes & Impacts* 18: 725–734.

671 Jolivet, C., Augusto, L., Trichet, P., Arrouays, D., 2007. Forest soils in the Gascony Landes Region: formation,
672 history, properties and spatial variability [WWW Document]. URL <http://hdl.handle.net/2042/8480>

673 Kerin, E.J., Gilmour, C.C., Roden, E., Suzuki, M.T., Coates, J.D., Mason, R.P., 2006. Mercury methylation by
674 dissimilatory iron-reducing bacteria. *Appl. Environ. Microbiol.* 72, 7919–7921.

675 Kostka, J.E., Luther, G.W., 1994. Partitioning and speciation of solid phase iron in saltmarsh sediments.
676 *Geochim. Cosmochim. Acta* 58: 1701–1710.

677 Lamborg, C.H., Fitzgerald, W.F., Damman, A.W.H., Benoit, J.M., Balcom, P.H., Engstrom, D.R., 2002. Modern
678 and historic atmospheric mercury fluxes in both hemispheres: Global and regional mercury cycling
679 implications. *Global. Biogeochem. Cycles* 16: 51-1– 51-11

680 MacDonald, D.D., Ingersoll C.G., Berger T.A., 2000. Development and evaluation of consensus-based
681 sediment quality guidelines for freshwater ecosystems. *Arch. Environ. Contam. Toxicol.* 39:
682 20–31.

683 Madison, A.S., Tebo, B.M., Luther, III G.W., 2011. Simultaneous determination of soluble manganese(III),
684 manganese(II) and total manganese in natural (pore)waters. *Talanta* 84: 374–381.

685 Mason, R.P., Fitzgerald, W.F., 1996. Sources, Sinks and Biogeochemical Cycling of Mercury in the Ocean. In:
686 Baeyens W, Ebinghaus R, Vasiliev O. (eds) *Global and Regional Mercury Cycles: Sources, Fluxes and*
687 *Mass Balances*, NATO ASI Series. Springer Netherlands, pp 249–272.

688 Mason, R.P., Fitzgerald, W.F., Morel, F.M.M., 1994. The biogeochemical cycling of elemental mercury:
689 Anthropogenic influences. *Geochim. Cosmochim. Acta* 58: 3191–3198.

690 Matty, J.M., Long, D.T., 1995. Early Diagenesis of Mercury in the Laurentian Great Lakes. *J. Great Lakes Res.*
691 21: 574–586.

692 Morel, F.M.M., Kraepiel, A.M.L., Amyot, M., 1998. The Chemical Cycle and Bioaccumulation of Mercury.
693 *Annu. Rev. Ecol. Syst.* 29: 543–566.

694 Myrbo, A., Swain, E.B., Johnson, N.W., Engstrom, D.R., Pastor, J., Dewey, B., Monson, P., Brenner, J.,
695 Dykhuizen Shore, M., Peters, E.B., 2017. Increase in nutrients, mercury, and methylmercury as a
696 consequence of elevated sulfate reduction to sulfide in experimental wetland mesocosms. *J. Geophys.*
697 *Res.: Biogeosciences* 122: 2769–2785.

698 Orem, W., Fitz, H.C., Krabbenhoft, D., Tate, M., Gilmour, C., Shafer, M., 2014. Modeling sulfate transport and
699 distribution and methylmercury production associated with Aquifer Storage and Recovery
700 implementation in the Everglades Protection Area. *Sustainability of Water Quality and Ecology* 3-4:
701 33–46.

702 Oremland, R.S., Culbertson, C.W., Winfrey, M.R., 1991. Methylmercury decomposition in sediments and
703 bacterial cultures: involvement of methanogens and sulfate reducers in oxidative demethylation
704 (English). *Appl. Environ. Microbiol.* 57:130–137.

705 Pak, K.R., Bartha, R., 1998. Mercury methylation and demethylation in anoxic lake sediments and by strictly
706 anaerobic bacteria. *Appl. Environ. Microbiol.* 64(3): 1013–1017.

707 Parks, J.M., Johs, A., Podar, M., Bridou, R., Hurt, R.A., Smith, S.D., Tomanicek, S.J., Qian, Y., Brown, S.D.,

708 Brandt, C.C., Palumbo, A.V., Smith, J.C., Wall, J.D., Elias, D.A., Liang, L., 2013. The genetic basis for
709 bacterial mercury methylation. *Science* 339, 1332–1335.

710 Pirrone, N., Cinnirella, S., Feng, X., Finkelman, R., Friedli, H., Leaner, J., Mason, R., Mukherjee, A., Stracher,
711 G., Streets, D., Telmer, K., 2010. Global mercury emissions to the atmosphere from anthropogenic and
712 natural sources. *Atmos. Chem. Phys.* 10 : 5951–5964.

713 Podar, M., Gilmour, C.C., Brandt, C.C., Soren, A., Brown, S.D., Crable, B.R., Palumbo, A.V., Somenahally,
714 A.C., Elias, D.A., 2015. Global prevalence and distribution of genes and microorganisms involved in
715 mercury methylation. *Sci. Adv.* 1(9):e1500675.

716 Ramlal, P.S., Kelly, C.A., Rudd, J.W.M., Furutani, A., 1993. Sites of Methyl Mercury Production in Remote
717 Canadian Shield. *Can. J. Fish. Aquat. Sci.* 50 : 972–979.

718 Renedo, R., Bustamante, P., Tessier, E., Pedrero, Z., Cherel, Y., Amouroux, D., 2017. Assessment of mercury
719 speciation in feathers using species-specific isotope dilution analysis. *Talanta* 174 : 100–110.

720 Rodier, J., 1976. *L'analyse de l'eau, eaux naturelles, eaux résiduaires, eau de mer.* Dunod, Paris.

721 Rodríguez Martín-Doimeadios, R.C., Tessier, E., Amouroux, D., Guyoneaud, R., Duran, R., Caumette, P.,
722 Donard, O.F.X., 2004. Mercury methylation/demethylation and volatilization pathways in estuarine
723 sediment slurries using species specific enriched stable isotopes. *Mar. Chem.* 90: 107-123.

724 Rolfhus, K.R., Sakamoto, H.E., Cleckner, L.B., Stoor, R.W., Babiarz, C.L., Back, R.C., Manolopoulos, H.,
725 Hurley, J.P., 2003. Distribution and fluxes of total and methylmercury in Lake Superior. *Environ. Sci.*
726 *Technol.* 37, 865e872.

727 Roustan, Y., Bocquet, M., Musson-Genon, L., Sportisse, B., 2006. Modélisation du mercure, du plomb et du
728 cadmium à l'échelle européenne. *Pollution Atmosphérique* 191: 317–326.

729 Schäfer, J., Castelle, S., Blanc, G., Dabrin, A., Masson, M., Lanceleur, L., Bossy, C., 2010. Mercury methylation
730 in the sediments of a macrotidal estuary (Gironde Estuary, south-west France). *Estuar. Coast. Shelf Sci.*
731 90: 80–92.

732 Schroeder, W.H., Munthe, J., 1998. Atmospheric Transport, Chemistry and Deposition of Mercury Atmospheric
733 mercury-An overview. *Atmos. Environ.* 32: 809–822.

734 Stookey, L.L., 1970. Ferrozine-a new spectrophotometric reagent for iron. *Anal Chem* 42: 779–781.

735 Streets, D.G., Horowitz, H.M., Jacob, D.J., Lu, Z., Levin, L., Ter Schure, A.F.H., Sunderland, E.M. 2017. Total
736 Mercury Released to the Environment by Human Activities, *Environ. Sci. Technol.* 51: 5969-5977.

737 Stumm, W., Morgan, J.J., 1996. *Aquatic chemistry*, 3rd ed. John Wiley & Sons.

738 United Nations Environment Programme (UNEP), 2013. *Global Mercury Assessment 2013: Sources, Emissions,*
739 *Releases and Environmental Transport.* Geneva.

740 Urban, N.R., Ernst, K., Bernasconi, S., 1999. Addition of sulfur to organic matter during early diagenesis of lake
741 sediments. *Geochim. Cosmochim. Acta* 63: 837–853.

742 Watras, C.J., Bloom, N.S., Claas, S.A., Morrison, K.A., Gilmour, C.C., Craig, S.R., 1995. Methylmercury
743 production in the anoxic hypolimnion of a dimictic seepage lake. *Water, Air, & Soil Pollut.* 80(1-4):
744 735-745.

745 Wedepohl, K.H., 1995. The composition of the continental crust. *Geochim. Cosmochim. Acta* 59: 1217–1232.

746

747

748 **Figure captions**

749 **Fig 1** Location map of Aquitaine coastal lakes and drainage basin land use. Small rings: Location of
750 river sampling for sulphate measurements; black star: location of soil sampling.

751 **Fig 2** Sediment mapping of Aquitaine lakes. Black dots and stars show the location of grab and core
752 samples in which Hg has been measured, respectively. Red dots are additional grabs that have been
753 collected to validate the sediment mapping based on bathymetry. The range of total carbon (TC)
754 concentrations and particulate total mercury (HgTp) levels for each sediment class is indicated in the
755 legend.

756 **Fig 3** Average grain size distribution of lake sandy sediment and catchment soils (right panel), and of
757 lake organic deposits after organic matter removal with H₂O₂ (left panel).

758 **Fig 4** Mean concentration of total carbon (TC), total sulphur (TS) and total Hg (HgTp) in organic
759 deposits (white bars) and in sandy sediments and catchment soils (grey bars) from the four Aquitaine
760 lakes. Error bars are standard deviations. Number of samples is indicated.

761 **Fig 5** Mean sulphate concentrations in streams that feed the lakes. Error bars are standard deviations.
762 Number of samples indicated in brackets. See Figure 1 for sampling location.

763 **Fig 6** Total Hg (HgTp) concentrations vs total sulphur (TS) concentrations in sediment grabs collected
764 in Aquitaine lakes.

765 **Fig 7** Relationship between the proportion (%) of MeHg relative to HgTp in organic sediments and
766 average sulphate concentrations in lake water column. Error bars are standard deviations (N=5 for
767 %MeHg, and N=15 for sulphate)

768

769

770

771

772

773

774

775

776

777

778

779

780

781

782

783

784

785
786
787

Table 1 Morpho-dynamics characteristics of Aquitaine lake.

Lake	Area (km ²)	Maximum depth (m)	Volume (10 ⁶ m ³)	Water residence time (year)	Elevation (m)	Catchment area (km ²)
Carcans-Hourtin	62	9	210	1.8	15	302
Lacanau	20	7	53	0.4	14	310
Cazaux-Sanguinet	58	23	498	4.3	21	200
Parentis-Biscarrosse	35	20.5	252	1	20	303

788
789
790
791
792

Table 2 Average mercury concentrations (mean total Hg, $\mu\text{g kg}^{-1}$ dry weight) in muscle of adult Perch (length 18-23 cm), Pike (>50 cm), and Zander (>50 cm) in the four lakes. Value \pm standard deviation; N: number of samples for different analysis.

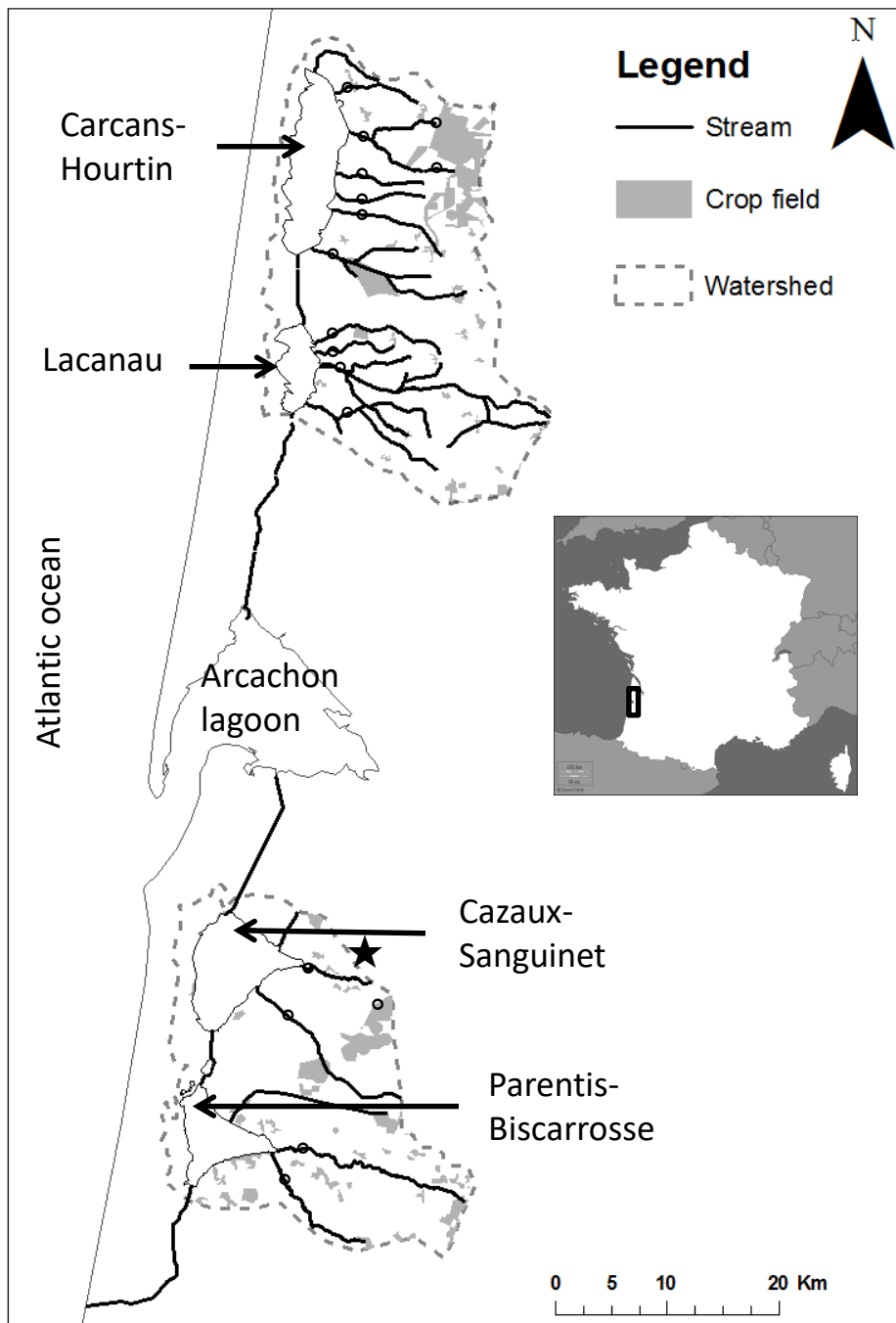
	Carcans-Hourtin	Lacanau	Cazaux-Sanguinet	Parentis-Biscarrosse
Perch (<i>Perca fluviatilis</i>)	1811 \pm 281 (N=6)	876 \pm 217 (N=7)	379 \pm 75 (N=16)	337 \pm 209 (N=4)
Pike (<i>Esox spp.</i>)	3151 \pm 1207 (N=8)	1608 \pm 752 (N=12)	1725 \pm 544 (N=7)	1459 \pm 333 (N=5)
Zander (<i>Sander lucioperca</i>)	6238 (N=1)	4809 (N=1)	3563 \pm 913 (N=6)	1642 \pm 485 (N=3)

797
798
799
800

Table 3 Total mercury (HgTp) and methyl mercury concentrations and methyl mercury fraction relative to HgTp of lake sediments and of SW France coastal sediments, and values reported in the literature.

Sediments	[HgTp] ($\mu\text{g kg}^{-1}$)	[MMHg _p] ($\mu\text{g kg}^{-1}$)	MMHg/HgTp (%)	References
Aquitaine lakes	100-420	1.1-5.1	0.5-2.5	This study
Arcachon Lagoon (SW France)	~ 200	~ 1	0.5	Bouchet et al., 2013
Gironde estuary (SW France)	~ 216	~ 0.7	0.3	Castelle, 2008
Everglades lakes (Florida)	50-400	<0.1-5	<0.2-2	Gilmour et al., 1998
Murray Lake (Papoua-New Guinea)	~ 111	~ 0.9	0.8	Bowles et al., 2001
St Lawrence River	~ 1500	~ 2.5	0.2	Avramescu et al., 2011
Lake Superior	83 \pm 12	0.21 \pm 0.03	<1	Rolfhus et al., 2003
Lake Titicaca	45-114	0.51-1.36	1.8 \pm 1.5	Guedron et al., 2017
Western North America lakes data base	29.3 \pm 6.5	0.55 \pm 0.05	0.9 \pm 0.1	Fleck et al., 2016

804
805
806



Sediment type

- Organic
- Sandy organic
- Organic sand
- Sand

TC(%)

- [10–30]
- [3–10]
- [1–3]
- [0–1]

HgTp ($\mu\text{g kg}^{-1}$)

- [100–420]
- [20–100]
- [4–20]
- [0–4]

